

1 **S100A8/A9 modulates inflammatory collateral tissue damage during**
2 **intraperitoneal origin systemic candidiasis**

3 Running title:

4 Calprotectin modulates collateral tissue damage

5 Authors:

6 Madhu Shankar^{*1,4}, Nathalie Uwamahoro^{*1}, Sandra Holmberg², Maria Joanna Niemiec^{1,5},
7 Johannes Roth³, Thomas Vogl³, Constantin F. Urban^{1#}

8 * Equally contributing first authors

9 # Corresponding author

10 Affiliations of authors:

11 ¹Department of Clinical Microbiology, Umeå Centre for Microbial Research (UCMR) &
12 Molecular Infection Medicine Sweden (MIMS), Umeå University, Umeå 90185, Sweden.

13 ²Department of Medical Chemistry and Biophysics, Umeå University, Umeå 90187, Sweden.

14 ³Institute of Immunology, Universitätsklinikum Münster & University of Münster, 48149
15 Münster, Germany

16 Current addresses:

17 ⁴ Department of Biochemistry & Molecular Biology, Monash Biomedicine Discovery Institute,
18 Melbourne, Australia

19 ⁵ Leibniz Institute for Natural Product Research and Infection Biology, Hans Knöll Institute
20 (HKI) & Center for Sepsis Control and Care, Jena, Germany

21 Full postal addresses of corresponding author:

22 Dr. Constantin F. Urban, Universitetssjukhuset by 6M, Department of Clinical Microbiology,

23 Immunology, Plan 4, Umeå universitet, 901 85 Umeå, Sweden, Phone: +46 90 785 27 02, Fax:

24 +46 90 12 99 05, Email: constantin.urban@umu.se

25 Keywords:

26 Sepsis, host-pathogen interactions, peritonitis, *Candida albicans*, inflammation

27

28 **Abstract**

29 Peritonitis is a leading cause of severe sepsis in surgical intensive care units, as over 70% of
30 patients diagnosed with peritonitis develop septic shock. A critical role of the immune system
31 is to return to homeostasis after combating infection. S100A8/A9 (calprotectin) is an
32 antimicrobial, pro-inflammatory protein complex often used as a biomarker for diagnosis of
33 disease activities in many inflammatory disorders. Here we describe the role of S100A8/A9 on
34 inflammatory collateral tissue damage (ICTD).

35 We performed an *in vivo* *Candida albicans* disseminated peritonitis mouse model using WT
36 and S100A9-deficient mice and stimulated primary macrophages with recombinant S100A8/A9
37 in the presence or absence of the compound paquinimod, a specific inhibitor of S100A9. In
38 addition, the effects on ICTD and fungal clearance were investigated. S100A9-deficient mice
39 developed less ICTD than wildtype mice. Restoration of S100A8/A9 in S100A9 knockout mice
40 resulted in increased ICTD and fungal clearance comparable to wildtype levels. Treatment with
41 paquinimod abolished ICTD.

42 The data indicated that S100A8/A9 controls ICTD levels and host antimicrobial modulation at
43 a systemic level during intra-abdominal candidiasis (IAC).

44

45 **Introduction**

46 Peritonitis frequently results in severe sepsis in surgical patients, especially in the intensive care
47 unit (ICU) (1), as more than 70% of patients often succumb to death within 72h (2). Hence,
48 treatment options are required that extend life expectancy to allow proper treatment (3).
49 Peritonitis is characterized by inflammation of the membrane in the abdominal cavity, the
50 peritoneum. Peritonitis often occurs upon disruption of physical barriers or can become
51 spontaneous in severe organ failure, causing alterations of the physiologic flora residing in the
52 gastrointestinal tract (1,4). These alterations prompt an inflammatory response that targets the
53 removal of contaminants from the peritoneal cavity into circulation. There, pathogens induce
54 activation of host immune responses and the release of pro-inflammatory mediators including
55 Interleukin-6 (IL6), macrophage inflammatory protein -1 α (MIP-1 α) and tumor necrosis factor
56 - α (TNF α) to recruit phagocytes to the peritoneum (5). The attempt to restrict infection
57 promotes abscess development through production of fibrinous exudate. Failure to confine
58 peritonitis may lead to organ failure, coma and death (6).

59 The inflammatory response of the innate immune system can either have intentional (pathogen
60 clearance) or collateral outcomes (pathological side effect, called inflammatory collateral tissue
61 damage -ICTD) (7). The focus of most studies on detection and elimination of pathogens has
62 neglected host tolerance to disease through the resolution of collateral outcomes of
63 inflammation in an attempt to establish homeostasis (8).

64 Acute or systemic inflammatory pathological states are often associated with intra-abdominal
65 surgery (9). Surgical intervention disrupting the natural barriers of the gastrointestinal tract
66 leads to deep-seated microbial infection by gut colonizing organisms and frequently *Candida*
67 *albicans* infection. As a result, the most common non-mucosal fungal diseases among
68 hospitalized patients are *Candida* peritonitis, also referred to as intra-abdominal candidiasis

69 (IAC). IAC is often challenging to diagnose and hence results in high mortality rates ranging
70 from 25% - 60% (9).

71 The resolution of infection is an active process involving reprogramming of cells and
72 modulation of mediators (10) such as the S100A8/A9 heterodimeric complex (calprotectin) also
73 known as alarmin or DAMP (11–13). Here, we used an experimental model for IAC to study
74 the contribution of S100A8/A9 to ICTD.

75 Participating as a signaling molecule that binds to Toll-like receptor-4 (TLR4) to induce pro-
76 inflammatory chemokines and cytokines, the heterodimer is the physiologically relevant and
77 active form that is secreted by activated, stressed or necrotic cells. The prolonged presence of
78 S100A8/A9, however, leads to a tolerated state of the immune system as a counter mechanism
79 or stress tolerance (12). Under high calcium conditions, such as present in the extracellular
80 milieu and culture medium, S100A8/A9 heterodimers inactivate itself by tetramer formation,
81 to restrict their activity locally and to avoid overwhelming immune reactions (13). Thus,
82 S100A8 homodimers, which cannot tetramerise, are widely accepted experimental stimuli to
83 mimic heterodimer activity.

84 Furthermore, S100A8/A9 binds micronutrients including zinc, manganese, and calcium, and is
85 often deployed by leukocytes as a mechanism to either deprive microbes of the nutrients or
86 poison the microbes in high quantities (14). Neutrophils release the heterodimer during the
87 formation of neutrophil extracellular traps to bind or capture *C. albicans* (15). In addition to the
88 antimicrobial benefit, S100A8/A9 is used in diagnostics to monitor neutrophil elevation in
89 various inflammatory diseases (16). The q-compound paquinimod, an immunomodulatory
90 compound that prevents the binding of S100A9 to TLR4, was designed to target chronic
91 inflammatory S100A8/A9 dependent diseases (17–22). Using a murine peritonitis model with
92 *C. albicans*, we show here that the inflammatory response failed to contain the pathogen in the
93 peritoneum but instead led to detrimental ICTD dependent on the presence of S100A8/A9.

94 Treatment of mice with paquinimod abrogated S100A8/A9-induced ICTD suggesting
95 paquinimod as promising adjunct therapy option during severe IAC.

96 **Materials and methods**

97 **Ethical statement**

98 Animal experiments and isolation of cells were carried out following the recommendations in
99 the Guide for the Care and Use of Laboratory Animals, conformed to Swedish animal protection
100 laws and applicable guidelines (djurskyddslagen 1988:534; djurskyddsförordningen 1988:539;
101 djurskyddsmyndigheten DFS 2004:4) in a protocol approved by the local Ethical Committee
102 (Umeå djurförsöksetiska nämnd, Permit number A12-13, A80-14 and A79-14).

103 **Statistical analyses**

104 Statistical analysis was conducted using Graphpad Prism 6 software and *P* values less than 0.5
105 were considered significant. All two-group comparisons in *Candida* CFU data, inflammatory
106 score, ALT data, and ELISA data were conducted using the unpaired, two-tailed student's *t*-
107 test. Comparisons of WT and *S100A9*^{-/-} mice data were performed using One-way ANOVA
108 multiple comparisons analysis as specified in figure legends. In all comparisons, the sample
109 size is specified in figure legends, and a *P*<0.05 was considered significant. **p*<0.05; ***p*<0.01;
110 ****p*<0.001; *****p*<0.0001.

111 **Yeast strains and growth conditions**

112 *C. albicans* clinical isolate strain - SC5314 was cultured overnight in YPD (1% yeast extract,
113 2% bacto-peptone and 2% glucose) at 30°C. The *Candida* cells were washed three times in PBS
114 prior use in all assays. Cell numbers were calculated using Vi-CELL Cell Viability Analyzer
115 (Beckman Coulter AB).

116 **Animal infections and isolation of bone marrow-derived macrophages, and tissue**
117 **analyses**

118 All mice were maintained according to a previous report (23) at Umeå Centre for Comparative
119 Biology (UCCB), Umeå University, Umeå, Sweden. If not otherwise stated mice were infected
120 intraperitoneally with 3×10^6 *C. albicans* cells per g mouse from an overnight culture in YPD.
121 For intravenous infection (only Fig. S4) mice were challenged intravenously with 2.5×10^3 *C.*
122 *albicans* cells per g mouse.

123 Primary macrophages (BMDMs) cells and differentiated as described in a previous
124 report (24). BMDMs flow cell cytometry (FACs) was conducted using BD LSR II flow
125 cytometer (BD Biosciences, San Jose, CA), using propidium iodide (24), on paquinimod treated
126 cells at indicated concentrations.

127 For tissue damage and fungal load, analyses were conducted according to a previous
128 report (25), with 3×10^6 *C. albicans* cells intraperitoneal injection per g of mouse after 24 hours
129 of infection (26). Blood ALT levels were measured using vetcscan VS2™ (SCIL animal care
130 company) as previously reported (27–29).

131 Histological preparations and inflammatory score analyses were conducted as in
132 previous reports (15,30). For the inflammatory score, Whole sections were analyzed for
133 inflammation and scored under the supervision of a specialized animal pathologist. The sections
134 from each animal were scored as zero if they had no inflammatory cells present in the tissue,
135 one for a few inflammatory cells (1–20 cells), two for moderate cell infiltration (21–40 cells),
136 three for a large number of inflammatory cells (41–60 cells), and four if inflammation was
137 spread all over in the tissue (61 cells) (30).

138 ***Cytokine and chemokine quantification***

139 BMDMs were seeded at 1×10^5 cells per well in 96-well microplates and then infected with *C.*
140 *albicans* at an MOI of 1 for 24 hours. Cell-free culture supernatants were harvested after *C.*

141 *albicans* infection. Supernatants were analyzed for indicated cytokines of chemokines by
142 ELISA (Biolegend-ELISA MAX™ 9727 Pacific Heights Blvd, San Diego, CA, USA), or Pro-
143 Mouse cytokine BioPlex® 200 multiplex (Bio-Rad Laboratories) according to the
144 manufacturer's instructions.

145 ***Generation of recombinant S100A8***

146 The S100A8 and S100A9 gene encoding for monomers of the mouse dimer S100A8/A9
147 (UniProt P27005, P31725) was synthesized, codon harmonized and purchased from DNA2.0.
148 The gene were GST tagged and cloned into *E. coli* BL21 strain. The cloned cells were auto-
149 induced overnight. The cells were pelleted and suspended in 10 mg/ml of 1×PBS supplemented
150 with DNase and protease inhibitors. The cells were lysed on ice by sonication (Branson Digital
151 sonifier; 10 mm horn, 50% power) for 6 min with alternating 10 s pulses and pauses. The lysate
152 was clarified by centrifugation at 23,000g for 20 min at 4°C. The clarified lysate was filtered
153 through a 0.45 µm syringe filter and batch bound to 2.0 ml GST sepharose (~25mg protein/ml)
154 for 2h at 4°C gravity flow over column and washed with 30 column volumes of PBS. Samples
155 were eluted in 4-6 ml fractions with 50 mM Tris pH 8 and 10 mM glutathione. For each fraction,
156 the resin was incubated with elution buffer for 10 min prior to collecting the flow through. The
157 fractions were analyzed at A280. The pooled fractions of protein were cleaved (1:100) using
158 protease 3c (PreScission®protease) to remove the GST tag and the fractions of GST tag free
159 protein were pooled. The protein was then separated by size-exclusion chromatography (SEC)
160 using a Superdex 75 16/600 column (GE Healthcare Life Sciences, UK) equilibrated with PBS
161 pH 7, at a flow rate of 0.5 ml/min. The fractions containing purified S100A8 (rA8) and S100A9
162 (rA9) were concentrated using an Amicon Ultra-4 centrifugal filter device with a 3 kDa
163 molecular-weight cutoff (Millipore). The primary sequence, the intact mass and the presence
164 of product were confirmed by mass spectrometry using an ABI 4800 MALDI tandem time-of-

165 flight mass spectrometer. Recombinant proteins were screened for endotoxin contamination and
166 levels were below 0.6 pg per μ g protein, as previously recommended (31).

167 **Results**

168 ***A disseminated fungal peritonitis model to determine roles of S100A8/A9***

169 During IAC, fungal cells dissemination reach the liver and other organs via lymphatics or
170 bloodstream (6). Liver tissue damage and leukocytosis are hallmarks of deep-seated and
171 systemic *C. albicans* infection (32). To establish a fungal IAC model and determine the role of
172 S100A8/A9 in systemic inflammation, we used *S100A9*-deficient mice (*S100A9*^{-/-}) that also
173 lack the S100A8 protein on the protein level despite normal S100A8 RNA level and thus
174 actually represent a functional S100A8/A9 double knockout mouse strain (33). Normally
175 expressed S100A8 protein in *S100A9*^{-/-} mice is rapidly degraded in the proteasome, avoiding
176 systemic overwhelming immune responses. However, under chronic TNF conditions, this
177 degradation process is insufficient leading to severe phenotypes in artificial mouse strains (TTP⁻
178 /^{-/-}*S100A9*^{-/-} or itghTNF/*S100A9*^{-/-}) indicating that heterodimer activity must be regulated
179 tightly to restrict operating range (13).

180 Using wildtype (WT) and *S100A9*^{-/-} mice, *C. albicans* intraperitoneal injections were
181 administered, liver tissues collected after 24 hours of infection and indicators of sepsis were
182 measured. The infection was determined to be systemic using phenotypic analysis of mice and
183 histopathological analysis from hematoxylin-eosin stained (H & E stain) liver sections after 24
184 hours. The development of eye exudates was an indication of fungal dissemination from the
185 peritoneal cavity to other loci in the mouse (Fig. 1A). WT liver sections indicated higher
186 numbers of leukocyte infiltration zones compared to *S100A9*^{-/-} sections (Fig. 1A, top panel).
187 Conversely, there was visual evidence of more fungal cells in the *S100A9*^{-/-} livers compared to
188 WT (Fig. 1A, bottom panel). The inflammatory score (Fig. 1B) showed a large number of

189 inflammatory cell infiltrates (level 3) in WT *C. albicans* infected samples compared to lack of
190 inflammation (level 1) observed in *S100A9*^{-/-} mice.

191 Blood alanine aminotransferase (ALT) levels in the blood are an indicator of liver damage
192 (1,29). *C. albicans* infected WT mice (101.6U/L) showed elevated levels compared to *S100A9*^{-/-}
193 mice (37.2U/L) which showed similar ALT levels to uninfected mice, suggesting lack of
194 systemic tissue damage in the S100A8/A9-deficient animals (Fig. 2A). The ability of the host
195 to clear the infection or organ microbial load is related to the colony-forming units (CFUs) (34).
196 *S100A9*^{-/-} mice had a significantly higher fungal load (2.5 fold of average levels) compared to
197 WT mice (Fig. 2B).

198 Macrophages are sentinels for immune signaling that leads to leukocytosis but may cause
199 problems when uncontrolled (35). The pro-inflammatory cytokine response of WT and *S100A9*^{-/-}
200 was determined using bone marrow-derived macrophages (BMDMs) to monitor the ability of
201 primary macrophages to induce TNF α (Fig. 2C). Higher levels of TNF α (3.1 fold of average
202 levels measured) upon *C. albicans* infection were induced by WT BMDMs (570 pg/ml)
203 compared to *S100A9*^{-/-} BMDMs (185 pg/ml), suggesting a defect in TNF α induction in cells
204 lacking S100A8/A9.

205 ***S100A8/A9 enhances pro-inflammatory cytokine release of macrophages***

206 The implications of the use of S100A8/A9 in recombinant protein therapy is unknown. To
207 determine whether the S100A8 activity would aid the *S100A9*^{-/-} mutant in eliciting an
208 appropriate cytokine response *in vitro*, BMDMs derived from S100A9-/- mice were infected
209 with *C. albicans* and treated with rS100A8. Murine *S100A8* was expressed in *E. coli*, purified
210 (Fig. S1) and verified by mass spectrometry to obtain functionally active homodimers as a
211 substitute for the heterodimer as previously reported (36). We included analyses for cytokines
212 typically released during early inflammatory responses (Fig. 3A-F).

213 Considerable increase of TNF α levels was obtained in *S100A9*^{-/-} BMDMs treated with
214 rS100A8 (Fig. 3A) comparable to WT levels upon *C. albicans* infection (Fig. 2C), and IL-6
215 was also strongly enhanced (Fig. 3B). In addition, *S100A9*^{-/-} BMDMs infected with *C. albicans*
216 and treated with rS100A8 released higher levels of chemokines *MIP1 α* (*CCL3*) and *MIP1 β*
217 (*CCL4*), crucial for the recruitment of various leukocyte subpopulations (Fig. 3C and 3D) as
218 compared to infected and untreated control macrophages. Also monitored was the induction of
219 the anti-inflammatory cytokine IL10, which showed low but significant levels induced when
220 mice were treated with rS100A8, while CXCL-1 levels declined (Fig. 3E and 3F). Induction of
221 pro-inflammatory cytokines and modulation of tissue damage by rS100A8 suggest that
222 S100A8/A9 heterodimers are main contributors of the acute pro-inflammatory response during
223 *C. albicans* infection.

224 ***Paquinimod reduces cytokine release of *C. albicans*-infected macrophages***

225 To potentially reduce ICTD during IAC pharmacological intervention blocking the pro-
226 inflammatory activity of S100A8/A9 could be used. Hence. the activity of paquinimod, a novel
227 anti-inflammatory compound initially developed against Systemic Lupus Erythematosus (SLE)
228 that targets S100A9, one subunit of the S100A8/A9 complex, in liver, lung, heart and skin (37),
229 was tested *in vitro*. The percentage of dead cells (propidium iodide positive cells) using flow
230 cytometry analysis (FACS) was assessed on treatment of WT BMDMs with various drug
231 concentrations of paquinimod. Among the concentrations used, no significant toxic effects were
232 observed (Fig. S2). However, there was significant TNF α reduction at 300 μ g/ml and 930 μ g/ml
233 paquinimod concentrations compared to untreated *C. albicans* infected BMDMs (Fig. 4A).
234 CCL-3 and IL-10 were also reduced upon addition of 930 μ g/ml paquinimod confirming the
235 activity for other cytokines and chemokines. Thus, paquinimod is likely able to block
236 S100A8/A9-mediated cytokine release during *C. albicans* infection.

237 ***S100A8/A9 is responsible for ICTD during disseminated peritonitis***

238 The active role of S100A8/A9 as alarmin during IAC is currently unknown. To test the
239 usefulness of recombinant protein therapy, we determined the effects of recombinant S100A8
240 protein (rS100A8) on disseminated *C. albicans* infection. Purified rS100A8 protein (100 μ l of a
241 100 μ g/ml solution) was injected into *C. albicans* infected WT and *S100A9*^{-/-} mice. Treatment
242 of *S100A9*^{-/-} mice with rS100A8 showed a higher level of ALT (5.9 fold of average levels
243 measured) compared to untreated with levels not significantly different to WT suggesting that
244 constitutively active S100A8 homodimers mimic heterodimers to cause WT levels of liver
245 damage (Fig. 5A) and that the S100A8/A9-mediated effect on ICTD is direct rather than
246 indirect. S100A8/A9 is an antimicrobial protein against *C. albicans* (15). In this context, the
247 fungal clearance defect observed in *C. albicans* infected *S100A9*^{-/-} mice was remedied, reducing
248 fungal load after treatment with rS100A8 (Fig. 5B).

249 ***Paquinimod therapy reduces ICTD induced by disseminated peritonitis***

250 Targeted deletion of *S100A9* improves survival in mouse models of bacterial-induced sepsis
251 (11,38). Higher lethality of a disseminated infection is often due to the inability to contain
252 inflammation-induced organ and tissue damage by the host (1). There are no specific
253 immunotherapies against disseminated infections, such as sepsis, and often management
254 focuses on containing the infection through source control and antibiotics or antifungals plus
255 organ function support (39). We hypothesized that using an anti-inflammatory drug in WT mice
256 may mimic the beneficial aspect (lack of tissue damage) observed in the *S100A9*^{-/-} mutant might
257 extend host survival from disseminated IAC. Treatment of intraperitoneally infected mice with
258 paquinimod led to complete elimination of ICTD as indicated by reduced ALT plasma levels
259 in infected mice to levels of uninfected mice (Fig. 5C). As expected, paquinimod treatment did
260 not have an effect on ALT levels in infected *S100A9*^{-/-} mice (Fig. 5C). In addition, paquinimod
261 treatment affected fungal burden in the liver of infected WT and *S100A9*^{-/-} mice only moderately

262 (Fig. 5D), probably due to reduced S100A8/A9-dependent activation of fungi-eliminating
263 immune cells. Of note, the CFU count in livers of *S100A9^{-/-}* mice was significantly higher than
264 in livers of WT mice, suggesting that ICTD after 24 h of infection is not strictly correlated to
265 fungal burden, but depends in this setting to a significant proportion on S100A8/A9 activity.

266 Paquinimod and other quinoline-3-carboxamides have been described as specific binders of
267 S100A9 (40). As rS100A9 does not form functional homodimers *in vitro* and hence could not
268 lead to a reduction of ICTD in experimental *C. albicans* peritonitis (Fig. S3), we used rS100A8.
269 Interestingly, the effect of rS100A8 injection on ALT plasma levels in infected *S100A9^{-/-}* mice
270 could be reverted by treatment with paquinimod (Fig. 5E), but expectedly had no effect on
271 fungal burden in the liver (Fig. 5F). It is possible that paquinimod binds recombinant mouse
272 S100A8 with somewhat higher affinity than recombinant human S100A8 which possibly could
273 explain the described effect.

274 ***Paquinimod has a moderate effect on survival in disseminated peritonitis***

275 To determine whether paquinimod could be used to alleviate sepsis derived from fungal
276 peritonitis, infected wildtype mice were treated with paquinimod every 24 hours with
277 paquinimod (Fig. 6A). The treatment resulted in a moderately increased survival rate after five
278 days post-infection with a statistically significant effect using log-rank test (Fig. 6B). Although
279 the compound did not prevent all mice from succumbing to systemic infection, between 24 and
280 48 hours treated mice survived longer compared to untreated mice (Fig. 6B). Despite the similar
281 weight loss in infected mice observed between treated and untreated groups (Fig. 6C), treated
282 mice were generally more active during *C. albicans* infection. Hence, our data suggest that anti-
283 S100A8/A9 therapy could be a useful strategy to increase the therapeutic window for antifungal
284 treatment during IAC, but probably could not serve as a standalone therapeutic approach.

285 **Discussion**

286 This work characterizes the role of immune-modulating S100A8/A9 on host resolution of
287 inflammation from a peritoneal-derived disseminated *C. albicans* infection. The gastrointestinal
288 commensal nature of *C. albicans* requires that mucosal damage and neutropenia are achieved
289 for *C. albicans* dissemination (41). Most experimental models studying systemic fungal
290 diseases use intravenous (IV) injection of fungal cells which bypass mucosal host defenses and
291 establish an infection predominantly in the kidney and in the brain (42). This study utilized an
292 IAC model to induce systemic inflammation mimicking a severe clinical concern of
293 postoperative *Candida* peritonitis (43). Similar to IV, IP-induced infection allows rapid blood
294 dissemination of pathogens with exposure to an active population of phagocytes, complement
295 cascade and the potential for abscess formation in the peritoneal cavity (43). The peritonitis
296 infection model presented here aimed to breach the immune barriers in the peritoneal cavity,
297 and this was phenotypically clear in the dissemination of *C. albicans* to the liver and to the eyes
298 of infected animals (Fig. 1 and 2). The IP injection route allows pathogen exposure to active
299 phagocyte populations in the peritoneum and the potential for the host to contain the infection
300 through the formation of abscesses (6). In intravenous infection, in contrast to the IP injection
301 route, ALT plasma level did not increase above uninfected control within the first 48 h of
302 infection (Fig. S4) and hence the peritonitis infection model is suitable to describe acute and
303 severe onset of disseminated infection leading to ICTD.

304 WT liver fungal clearance was ~3 times more efficient when compared to the S100A8/A9-
305 deficient mice (Fig. 2B). The various leucocyte infiltration zones observed in WT liver tissues
306 compared to *S100A9*^{-/-} mice (Fig. 1A) indicated that the recruitment of higher levels of
307 leukocytes coincides with fungal clearance in WT mice. These findings suggested that the
308 presence of S100A8/A9 is required for fungal clearance during disseminated infection, and
309 supports our previous findings that implicated antimicrobial properties of S100A8/A9 during

310 candidiasis (15). Notably, presence of S100A8/A9 in WT mice resulted to significantly more
311 liver damage compared to *S100A9^{-/-}* mice as indicated by ALT plasma levels despite higher
312 fungal load in the liver (Fig. 2A and B), implicating that the induction of S100A8/A9
313 inflammatory responses modulates processes which contribute to tissue damage. These findings
314 support the association of the S100 family of proteins with inflammatory disorders (13), and
315 our data indicate that S100A8/A9 activity depends on modulation of both antimicrobial and
316 inflammatory activity. These insights would especially be critical in the case of
317 immunocompromised patients.

318 The IP treatment with rS100A8 of *C. albicans*-infected *S100A9^{-/-}* mice resulted in fungal
319 clearance similar to WT mice. Since rS100A8 showed significant *in vivo* activity, we used
320 *S100A9^{-/-}* bone marrow-derived macrophages in a *C. albicans* *ex vivo* infection assay, and
321 showed that rS100A8 mediates macrophage activation as indicated by the higher levels of the
322 chemokines CCL-3 and CCL-4, pro-inflammatory cytokines IL-6 and TNF α , as well as the
323 anti-inflammatory cytokine IL10 (Fig. 3). The induction of IL10 by rS100A8 is consistent with
324 homeostatic management of systemic inflammation (44). Balancing of pro- and anti-
325 inflammatory cytokines is a common theme of host factors with local and system-wide effects
326 as exemplified by interferon signaling pathways during viral infections (45). Albeit
327 administration of rS100A8 led to enhanced fungal clearance in the liver of infected S100A8/A9-
328 deficient mice, the activity of S100A8 has the potential to induce dire effects on host-mediated
329 tissue damage which probably do not warrant recombinant therapy with rS100A8 in
330 immunocompromised individuals.

331 Our data demonstrate that ICTD, which was alleviated in S100A8/A9-deficient mice, could be
332 fully reintroduced by injection of recombinant protein (rS100A8). Thus, the reported effect on
333 ICTD in an experimental model of IAC is, at least to a large proportion, dependent on
334 S100A8/A9 and pharmacological targeting of the protein complex could be beneficial in

335 patients with IAC. To demonstrate this, we used paquinimod; a compound applied for treatment
336 of chronic inflammatory diseases (17,20). As paquinimod is a specific binder for S100A9 (40),
337 it blocks the pro-inflammatory activity of the S100A8/A9 complex *in vivo*. Surprisingly, we
338 found that paquinimod also reverted ICTD in infected S100A9/- mice previously treated with
339 rS100A8 (Fig. 5E). Bjork *et al.*, showed strong binding of paquinimod to human and mouse
340 S100A9 and negligible binding to human S100A8 *in vitro*; however, binding to mouse S100A8
341 was not investigated (40). Notably, it may also be possible that paquinimod exerts other
342 immune-modulatory effects that give rise to the reduction seen in Fig. 5E. No toxicity was
343 observed against bone marrow-derived macrophages (BMDMs) at the concentration used in
344 animal infection experiments and paquinimod activity affected the inflammatory modulators as
345 observed in the reduction of CCL-3 and IL-10. No adverse effects on fungal load in livers of
346 infected animals were seen either (Fig. 5D). Hence, paquinimod represents a potential adjuvant
347 therapeutic option that dampens the host responses to avoid tissue damage and increases the
348 therapeutic window (Fig. 6B) for targeting the pathogen with antifungal drugs, in particular,
349 since the compound had no adverse effect on fungal clearance.

350 This study showed the dilemma of the protective and harmful roles of S100A8/A9 in *Candida*
351 *albicans*-induced fungal peritonitis (Fig. 6). Fungal peritonitis that is not contained by host
352 defenses leads to pathogen infiltration of host organs (Fig. 7.1). Fungal-host interaction induces
353 the systemic release of S100A8/A9 (15) for fungal clearance and ALTs into the systemic
354 circulation (Fig. 7.2-7.3). Local innate immune cells (represented in this study as primary
355 macrophages respond with a cytokine ‘storm’ of pro-inflammatory cytokines (Fig. 7.4-7.5), that
356 leads to increased leukocyte infiltrates systemically (Fig. 7.6), and promote increased tissue
357 damage in the effort of fungal clearance (Fig. 7.7). Hence, our study presents both the potential
358 for a systemically functional protein, evidence for potential antimicrobial recombinant protein
359 therapy, and adjuvant treatment as paquinimod-mediated inhibition of S100A8/A9 showed

360 reduction of ICTD (Fig. 7). Considering the high mortality (>50%) due to do fungal sepsis (1),
361 future adjuvant therapies similar to paquinimod could be the key against peritonitis and other
362 severe inflammatory malignancies.

363

364 **Acknowledgments**

365 The authors thank José Pedro Lopes and Sujan Yellagunda for support with animal experiments.
366 We acknowledge essential advice and the kind gift of paquinimod from Active Biotech. We
367 acknowledge support for heterologous protein expression of the Protein Expertise Platform
368 (PEP) at Umeå University. Furthermore, we are grateful for funding provided to CFU by the
369 Swedish research council VR-M 2014-02281 and VR-M 2017-01681, the Kempe Foundation
370 SMK-1453, the Åke Wiberg Foundation M14-0076 and M15-0108, and the Medical Faculty of
371 Umeå University 316-886-10. NU and MS held a postdoctoral fellowship received in
372 competition from UCMR. The funders had no rule in study design nor analysis and
373 interpretation of the results.

374 **Author Contribution**

375 CFU provided funding and together with MS and NU designed the study, MS and NU collected
376 and analyzed the data. TV and JR contributed to the conceptualization of the study. Manuscript
377 drafting by NU, MS and CFU. SH contributed preparation of histological sections. MJN
378 provided data from intravenous infection. All authors contributed to data analysis, drafting and
379 critically revising the paper, gave final approval of the version to be published, and agree to be
380 accountable for all aspects of the work.

381 **Conflict of interest**

382 The authors declare no conflict of interest.

383

384 **References**

- 385 1. Fiore M, Maraolo AE, Leone S, Gentile I, Cuomo A, Schiavone V, Bimonte S, Pace MC,
386 Cascella M. Spontaneous peritonitis in critically ill cirrhotic patients: a diagnostic algorithm for
387 clinicians and future perspectives. *Ther Clin Risk Manag* (2017) **13**:1409–1414.
388 doi:10.2147/TCRM.S144262
- 389 2. Paoli C, Reynolds M, Sinha M, Gitlin M. 1486: Current burden, Outcomes, and Costs of Sepsis
390 Management in United States hospitals. *Crit Care Med* (2018) **46**:
- 391 3. Denning DW, Perlin DS, Muldoon EG, Colombo AL, Chakrabarti A, Richardson MD, Sorrell
392 TC. Delivering on Antimicrobial Resistance Agenda Not Possible without Improving Fungal
393 Diagnostic Capabilities. *Emerg Infect Dis J* (2017) **23**:177. doi:10.3201/eid2302.152042
- 394 4. de Jong PR, González-Navajas JM, Jansen NJG. The digestive tract as the origin of systemic
395 inflammation. *Crit Care* (2016) **20**:279. doi:10.1186/s13054-016-1458-3
- 396 5. Yao V, Platell C, Hall JC. Role of peritoneal mesothelial cells in peritonitis. *BJS (British J*
397 *Surgery)* (2003) **90**:1187–1194. doi:10.1002/bjs.4373
- 398 6. Skipworth RJE, Fearon KCH. Acute abdomen: peritonitis. *Surg* (2008) **26**:98–101.
399 doi:<https://doi.org/10.1016/j.mpsur.2008.01.004>
- 400 7. Wang A, Huen SC, Luan HH, Yu S, Zhang C, Gallezot J-D, Booth CJ, Medzhitov R. Opposing
401 Effects of Fasting Metabolism on Tissue Tolerance in Bacterial and Viral Inflammation. *Cell*
402 (2016) **166**:1512–1525.e12. doi:10.1016/j.cell.2016.07.026
- 403 8. Hamidzadeh K, Christensen SM, Dalby E, Chandrasekaran P, Mosser DM. Macrophages and
404 the Recovery from Acute and Chronic Inflammation. *Annu Rev Physiol* (2017) **79**:567–592.
405 doi:10.1146/annurev-physiol-022516-034348
- 406 9. Lichtenstern C, Schmidt J, Knaebel HP, Martin E, Büchler MW, Weigand MA. Postoperative
407 Bacterial/Fungal Infections: A Challenging Problem in Critically Ill Patients after Abdominal
408 Surgery. *Dig Surg* (2007) **24**:1–11. doi:10.1159/000099009
- 409 10. Netea MG, Balkwill F, Chonchol M, Cominelli F, Donath MY, Giamarellos-Bourboulis EJ,
410 Golenbock D, Gresnigt MS, Heneka MT, Hoffman HM, et al. A guiding map for inflammation.
411 *Nat Immunol* (2017) **18**:826–831. doi:10.1038/ni.3790
- 412 11. Vogl T, Tenbrock K, Ludwig S, Leukert N, Ehrhardt C, van Zoelen MAD, Nacken W, Foell D,
413 van der Poll T, Sorg C, et al. Mrp8 and Mrp14 are endogenous activators of Toll-like receptor
414 4, promoting lethal, endotoxin-induced shock. *Nat Med* (2007) **13**:1042–1049.
415 doi:10.1038/nm1638
- 416 12. Austermann J, Friesenhagen J, Fassl SK, Ortakas T, Burgmann J, Barczyk-Kahlert K, Faist E,
417 Zedler S, Pirr S, Rohde C, et al. Alarmins MRP8 and MRP14 Induce Stress Tolerance in
418 Phagocytes under Sterile Inflammatory Conditions. *Cell Rep* (2014) **9**:2112–2123.
419 doi:<https://doi.org/10.1016/j.celrep.2014.11.020>
- 420 13. Vogl T, Stratis A, Wixler V, Völler T, Thurainayagam S, Jorch SK, Zenker S, Dreiling A,
421 Chakraborty D, Fröhling M, et al. Autoinhibitory regulation of S100A8/S100A9 alarmin
422 activity locally restricts sterile inflammation. *J Clin Invest* (2018) **128**:1852–1866.
423 doi:10.1172/JCI89867
- 424 14. Zackular JP, Chazin WJ, Skaar EP. Nutritional Immunity: S100 Proteins at the Host-Pathogen
425 Interface. *J Biol Chem* (2015) **290**:18991–18998. doi:10.1074/jbc.R115.645085
- 426 15. Urban CF, Ermert D, Schmid M, Abu-Abed U, Goosmann C, Nacken W, Brinkmann V,
427 Jungblut PR, Zychlinsky A. Neutrophil extracellular traps contain calprotectin, a cytosolic
428 protein complex involved in host defense against *Candida albicans*. *PLoS Pathog* (2009)

429 5:e1000639–e1000639. doi:10.1371/journal.ppat.1000639

430 16. Chan JK, Roth J, Oppenheim JJ, Tracey KJ, Vogl T, Feldmann M, Horwood N, Nanchahal J.
431 Alarmins: awaiting a clinical response. *J Clin Invest* (2012) **122**:2711–2719.
432 doi:10.1172/JCI62423

433 17. Fransén Pettersson N, Deronic A, Nilsson J, Hannibal TD, Hansen L, Schmidt-Christensen A,
434 Ivars F, Holmberg D. The immunomodulatory quinoline-3-carboxamide paquinimod reverses
435 established fibrosis in a novel mouse model for liver fibrosis. *PLoS One* (2018) **13**:e0203228–
436 e0203228. doi:10.1371/journal.pone.0203228

437 18. Kraakman MJ, Lee MK, Al-Sharea A, Dragoljevic D, Barrett TJ, Montenont E, Basu D,
438 Heywood S, Kammoun HL, Flynn M, et al. Neutrophil-derived S100 calcium-binding proteins
439 A8/A9 promote reticulated thrombocytosis and atherogenesis in diabetes. *J Clin Invest* (2017)
440 **127**:2133–2147. doi:10.1172/JCI92450

441 19. Masouris I, Klein M, Dyckhoff S, Angele B, Pfister HW, Koedel U. Inhibition of DAMP
442 signaling as an effective adjunctive treatment strategy in pneumococcal meningitis. *J*
443 *Neuroinflammation* (2017) **14**:214. doi:10.1186/s12974-017-0989-0

444 20. Schelbergen RF, Geven EJ, van den Bosch MHJ, Eriksson H, Leanderson T, Vogl T, Roth J,
445 van de Loo FAJ, Koenders MI, van der Kraan PM, et al. Prophylactic treatment with S100A9
446 inhibitor paquinimod reduces pathology in experimental collagenase-induced osteoarthritis.
447 *Ann Rheum Dis* (2015) **74**:2254 LP – 2258. doi:10.1136/annrheumdis-2014-206517

448 21. van den Bosch MH, Blom AB, Schelbergen RF, Koenders MI, van de Loo FA, van den Berg
449 WB, Vogl T, Roth J, van der Kraan PM, van Lent PL. Alarmin S100A9 Induces
450 Proinflammatory and Catabolic Effects Predominantly in the M1 Macrophages of Human
451 Osteoarthritic Synovium. *J Rheumatol* (2016) **43**:1874 LP – 1884. doi:10.3899/jrheum.160270

452 22. Yun J, Xiao T, Zhou L, Beuerman RW, Li J, Zhao Y, Hadayer A, Zhang X, Sun D, Kaplan HJ,
453 et al. Local S100A8 Levels Correlate With Recurrence of Experimental Autoimmune Uveitis
454 and Promote Pathogenic T Cell Activity. *Invest Ophthalmol Vis Sci* (2018) **59**:1332–1342.
455 doi:10.1167/iovs.17-23127

456 23. Hobbs JAR, May R, Tanousis K, McNeill E, Mathies M, Gebhardt C, Henderson R, Robinson
457 MJ, Hogg N. Myeloid cell function in MRP-14 (S100A9) null mice. *Mol Cell Biol* (2003)
458 **23**:2564–2576. doi:10.1128/mcb.23.7.2564-2576.2003

459 24. Uwamahoro N, Verma-Gaur J, Shen H-H, Qu Y, Lewis R, Lu J, Bamberg K, Masters SL,
460 Vince JE, Naderer T, et al. The Pathogen Candida albicans Hijacks Pyroptosis for Escape from
461 Macrophages. *MBio* (2014) **5**:e00003-14. doi:10.1128/mBio.00003-14

462 25. Lopes JP, Stylianou M, Backman E, Holmberg S, Jass J, Claesson R, Urban CF. Evasion of
463 Immune Surveillance in Low Oxygen Environments Enhances Candida albicans Virulence.
464 *MBio* (2018) **9**:e02120-18. doi:10.1128/mBio.02120-18

465 26. Vethanayagam RR, Almyroudis NG, Grimm MJ, Lewandowski DC, Pham CTN, Blackwell
466 TS, Petraitiene R, Petraitis V, Walsh TJ, Urban CF, et al. Role of NADPH Oxidase versus
467 Neutrophil Proteases in Antimicrobial Host Defense. *PLoS One* (2011) **6**:e28149. Available at:
468 <https://doi.org/10.1371/journal.pone.0028149>

469 27. Parasuraman S, Raveendran R, Kesavan R. Blood sample collection in small laboratory
470 animals. *J Pharmacol Pharmacother* (2010) **1**:87–93. doi:10.4103/0976-500X.72350

471 28. Röhm M, Grimm MJ, D'Auria AC, Almyroudis NG, Segal BH, Urban CF. NADPH oxidase
472 promotes neutrophil extracellular trap formation in pulmonary aspergillosis. *Infect Immun*
473 (2014) **82**:1766–1777. doi:10.1128/IAI.00096-14

474 29. Vatsalya V, Avila D, Frimodig JC, Barve SS, McClain CJ, Gobejishvili L. Liver Injury

521 44. Shouval DS, Ouahed J, Biswas A, Goettel JA, Horwitz BH, Klein C, Muise AM, Snapper SB.
522 Interleukin 10 receptor signaling: master regulator of intestinal mucosal homeostasis in mice
523 and humans. *Adv Immunol* (2014) **122**:177–210. doi:10.1016/B978-0-12-800267-4.00005-5

524 45. Majer O, Bourgeois C, Zwolanek F, Lassnig C, Kerjaschki D, Mack M, Müller M, Kuchler K.
525 Type I interferons promote fatal immunopathology by regulating inflammatory monocytes and
526 neutrophils during *Candida* infections. *PLoS Pathog* (2012) **8**:e1002811–e1002811.
527 doi:10.1371/journal.ppat.1002811

528

529 **Figure Legends**

530 **Figure 1. Disseminated *C. albicans* peritonitis mouse model depicting the necessity of**
531 **S100A8/A9 in inflammation.** Intraperitoneal (IP) *C. albicans* infection (3×10^6 cells per g
532 mouse) in WT or S100A8/A9-deficient mice after 24 hours. **A)** Fungal eye exudate as evidence
533 for peritoneal cavity failure to contain *C. albicans* infection after 24. Shown is the clear eye of
534 uninfected (PBS) compared to the white pus in infected wild type (WT) mouse. **B)**
535 Representative photomicrographs of hematoxylin-eosin (H&E) stained liver sections of
536 uninfected and infected wildtype and s100A9 mutant used in quantifications in **C**). Zoomed
537 images show one of many observed increased inflammatory cell infiltrates in WT infected cells
538 (top panel), and arrows indicate yeast or hyphal cells (bottom panel) at 20x magnification. CV:
539 central vein, PV: portal vein. **C)** An inflammatory score of H&E-stained liver sections of
540 uninfected and infected WT and S100A9^{-/-} mutant mice. A score of 2 = moderate cell
541 infiltration, >3 = large number of infiltrates, 4 = full tissue inflammatory infiltration. Data from
542 10x microscopy image fields of 2 sections from mice n=2 (WT and *S100A9* ^{-/-}) and n=6 (WT
543 + Ca and *S100A9* ^{-/-} + Ca). Error bars indicate standard deviation and ***p< 0.0001

544 **Figure 2. S100A8/A9 is required for inflammatory induced collateral tissue damage**
545 **(CTD) and fungal clearance in the liver. A-B)** WT and S100A9^{-/-} mice were infected with 3×10^6 cells per g of mice. **A)** Alanine transferase levels (ALTs) used as an indicator of liver
546 tissue damage as a result of *C. albicans* infection. Plasma ALT levels were analyzed from 100 μ l
547 of plasma in a vetcscan rotor 24 h post-infection. **B)** Organ levels of colony-forming units
548 (CFUs) as a measure of host fungal burden. *C. albicans* CFUs in homogenized infected livers
549 of indicated mice were quantified. **A-B)** Box- and whisker plots show the smallest observation,
550 lower quartile, mean, upper quartile and largest observation. n = 7 (WT and S100A9^{-/-}), and
551 n= 10 (WT and S100A9^{-/-} + Ca) total mice. **** p-value = <0.0001. **C)** *C. albicans* *in vitro*
552 infection of immune cells induces the production of less pro-inflammatory cytokines. WT and

554 S100A9-/- bone marrow-derived macrophages (BMDMs) were infected with *C. albicans* (MOI
555 1). TNF α levels were measured from supernatants at 24-hour post-infection. ** p-value = <0.01,
556 n = 3.

557 **Figure 3. Recombinant S100A8 protein restores pro-inflammatory cytokine release of**
558 ***S100A9*^{-/-} bone marrow-derived macrophages upon *in vitro* *C. albicans* infection.** Cytokine
559 levels **A)** TNF α , **B)** LI-6, **C)** CCL3, **D)** CCL-4, **E)** IL-10, and **F)** CXCL-1 in supernatants of
560 bone marrow-derived macrophages (BMDMs) infected with *C. albicans* (MOI 1) were
561 measured 24-hour post-infection. A Pro-Mouse cytokine BioPlex[®] 200 multiplex array (Bio-
562 Rad, Hercules, CA) was used to detect and quantify *S100A9*^{-/-} mouse cytokines infected with
563 *C. albicans* with and without additional treatment with rS100A8 (10 μ g/ml). **A-F)** n=3, *p-
564 value = <0.05 ****p-value = <0.0001.

565 **Figure 4. Quinoline-3-carboxamide paquinimod (Paq) reduces pro-inflammatory**
566 **cytokine release of WT bone marrow-derived macrophages upon *in vitro* *C. albicans***
567 **infection. A)** WT BMDM were infected and treated with different Paq concentrations
568 (930 μ g/ml – 12.5 μ g/ml). TNF α was measured from supernatants 24 h post-infection. **B-C)** WT
569 BMDM were infected and treated with 930 μ g/ml or 0 μ g/ml Paq and release of B) CCL-3 and
570 C) IL-10 was measured from supernatants after 24 h. **A-C)** n=3. *p-value = <0.05, ****p-value
571 = <0.0001.

572 **Figure 5. Recombinant S100A8 and paquinimod modify collateral tissue damage in**
573 **experimental disseminated *C. albicans* peritonitis. A)** Effect of recombinant soluble
574 rS100A8 on *C. albicans* induced collateral tissue damage. Protein was intraperitoneally
575 administered (approximately 10 μ g per mouse) to WT and *S100A9*^{-/-} mice intraperitoneally
576 infected with *C. albicans* (3×10^6 cells per g mouse) and shown are plasma ALT levels. **B)**
577 Effect of rS100A8 on host fungal clearance. Shown are CFUs from homogenized infected livers
578 of indicated mice **A-B)** Data are presented as a box- and whisker plots showing the smallest

579 observation, lower quartile, mean, upper quartile and largest observation, statistical significance
580 was analyzed by one-way ANOVA n = 5 mice per group in 3 separate experiments, ***p-
581 value = <0.0001. **C-D)** Effects of paquinimod (Paq) on *C. albicans*-induced collateral tissue
582 damage and fungal clearance in intraperitoneally infected mice. Paq was administered
583 intraperitoneally (30mg/kg). Shown are plasma ALT levels **C)** and CFUs from homogenized
584 infected livers **D)** from *C. albicans* infected WT and *S100A9*^{-/-} mice. **E-F)** Effect of Paq on
585 recombinant S100A8/A9 induced collateral tissue damage during *C. albicans* infection. Note
586 that **E)** contains *S100A9*^{-/-} controls initially presented in **A)** as experiments were conducted
587 together. Shown are plasma ALT levels **E)** and CFUs from homogenized infected livers **F)**
588 from *C. albicans* infected *S100A9*^{-/-} mice treated with rS100A8 (10 μ g per mouse) with or
589 without Paq treatment. Data are presented as a box- and whisker plots showing the smallest
590 observation, lower quartile, mean, upper quartile and largest observation, statistical significance
591 was analyzed by student t-test n = 5 mice per group, *p-value = <0.05, ***p-value = <0.0001.

592 **Figure 6. Inhibition of S100A8/A9 by paquinimod moderately increases host survival**
593 **from disseminated *C. albicans* peritonitis A-D)** WT mice infected with *C. albicans* were
594 treated with Paq (30mg/kg) at 24-hour intervals up to 5 days, and mice weight and survival
595 were monitored. **A)** Paq mice treatment strategy. **B** Survival B) and sequential body weight C)
596 of WT mice infected and treated at the indicated timeline. Survival is moderately but
597 significantly increased. n = 8 mice per group. For survival log-rank test p-value = 0.0169, for
598 mouse weight grams lost over time is shown. **p-value <0.01. Shown are mean and SD.

599 **Figure 7. Study summary.** Using a systemic fungal peritonitis mouse model (1), findings
600 implicate S100A8/A9 as a systemically essential protein (2-6, i-vi)) for the control of cytokine
601 and chemokine modulation (4-5), organ leukocyte recruitment (6), host tissue damage (7) and
602 fungal clearance (vi). In systemic intra-abdominal originating candidiasis, the cost of fungal
603 clearance (antimicrobial/active S100A8/A9 signaling) a feedback-loop that increases tissue

604 damage, while the cost of decreased tissue damage (anti-inflammatory/ inactive S100A8/A9
605 signaling) is a higher fungal burden (Fig. 1-5). Both are lethal if not controlled (Fig. 5B). Future
606 studies should focus on fine-tuning recombinant therapy in cases where active S100A8/A9
607 signaling is inadequate, and anti-inflammatory treatments like paquinimod, in conjunction with
608 antifungal treatments to increase host survival time to aid treatment.

609

Figure 1 (Shankar et al. 2020)

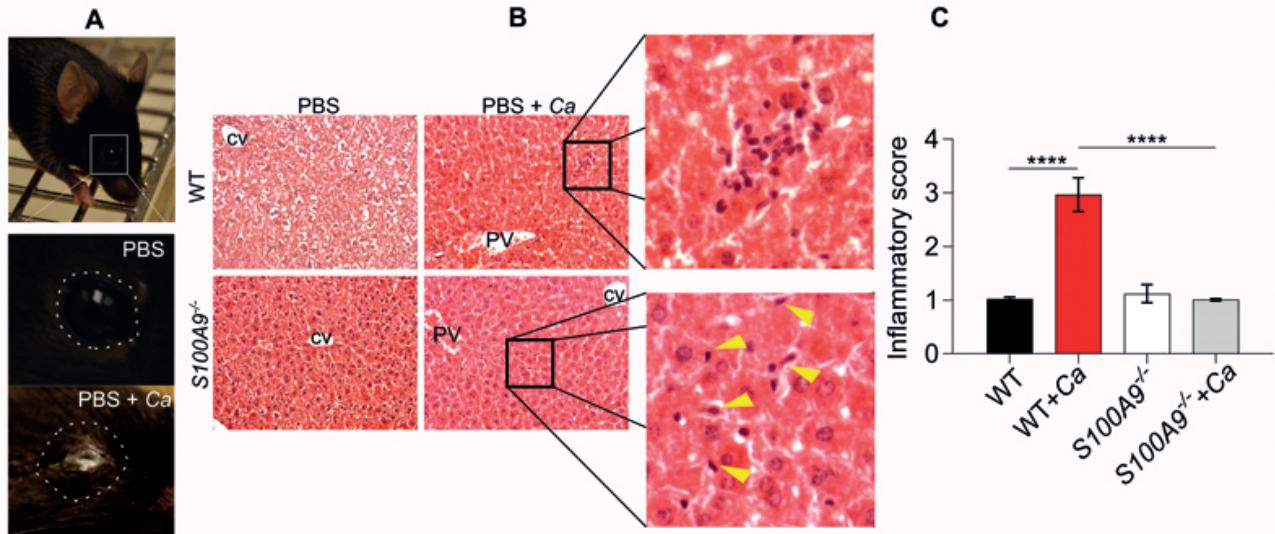


Figure 2 (Shankar et al. 2020)

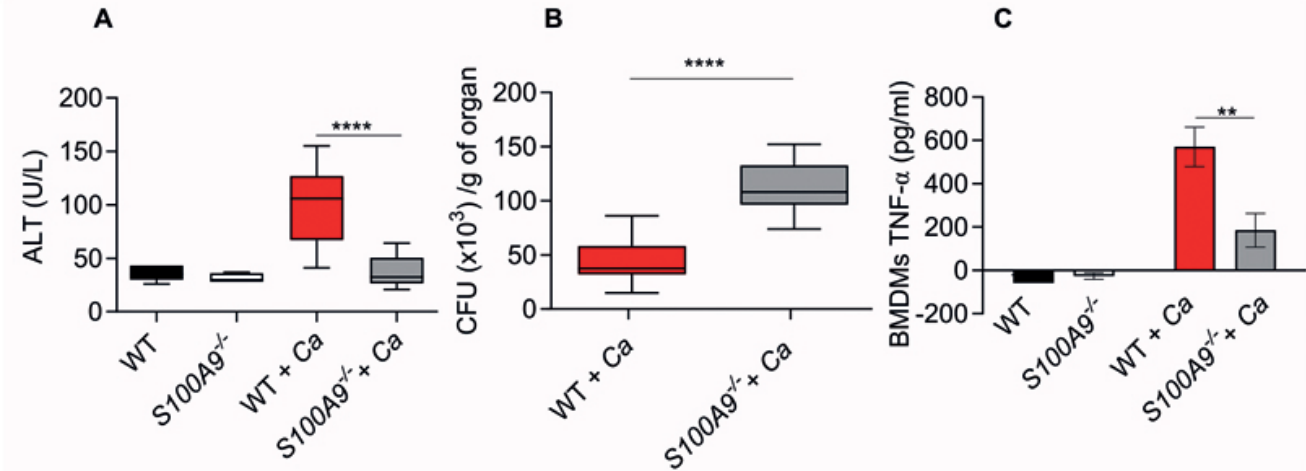


Figure 3 (Shankar et al. 2020)

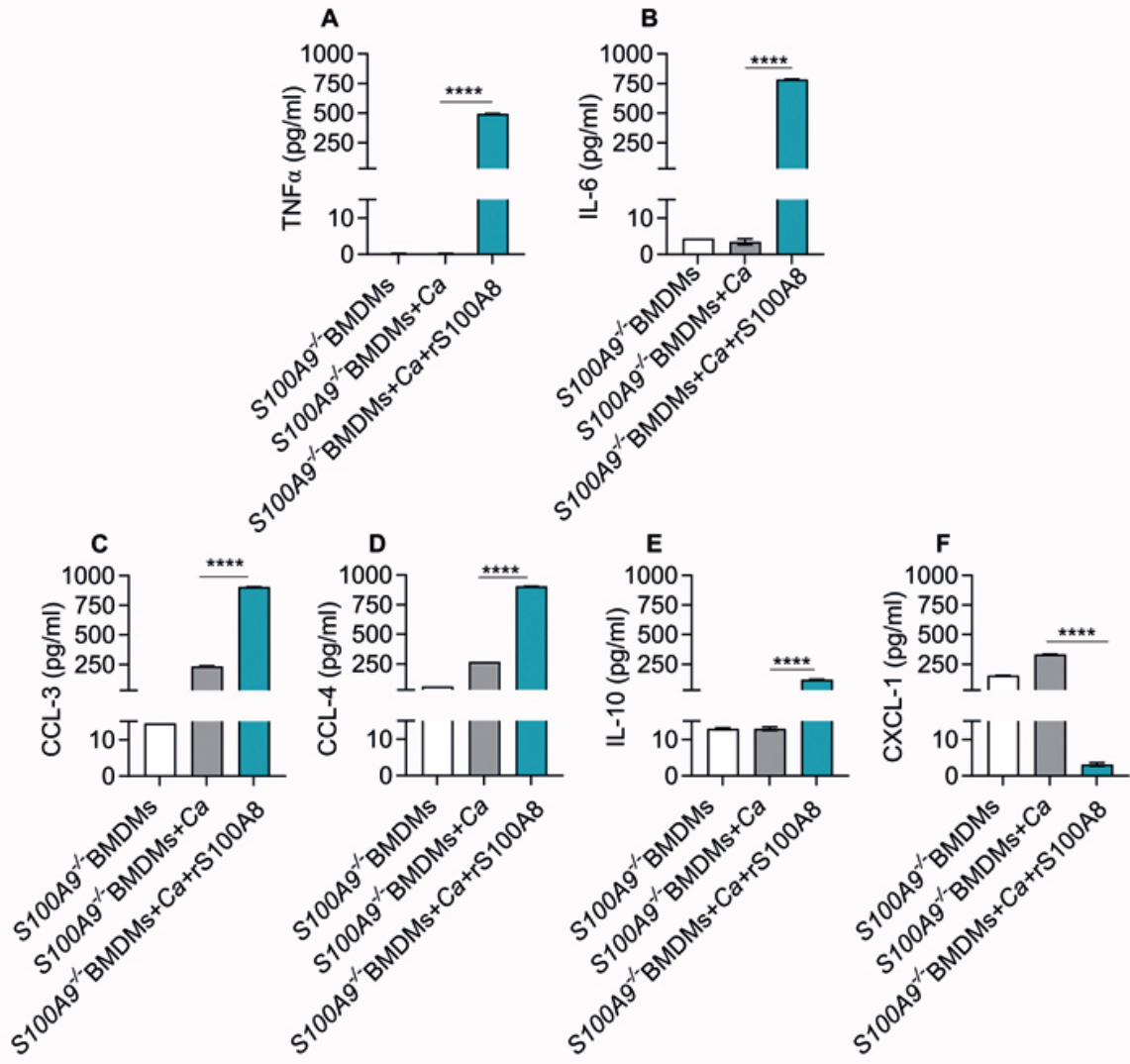


Figure 4 (Shankar et al. 2020)

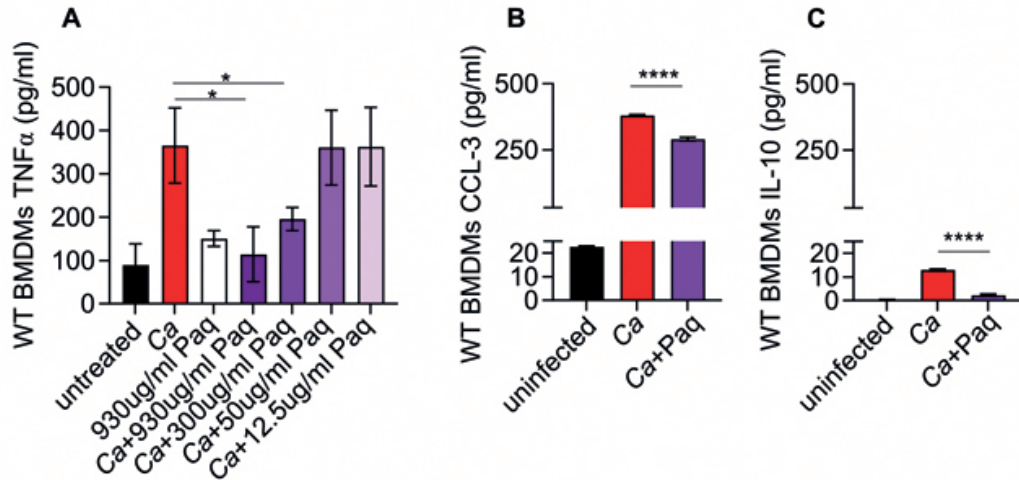


Figure 5 (Shankar et al. 2020)

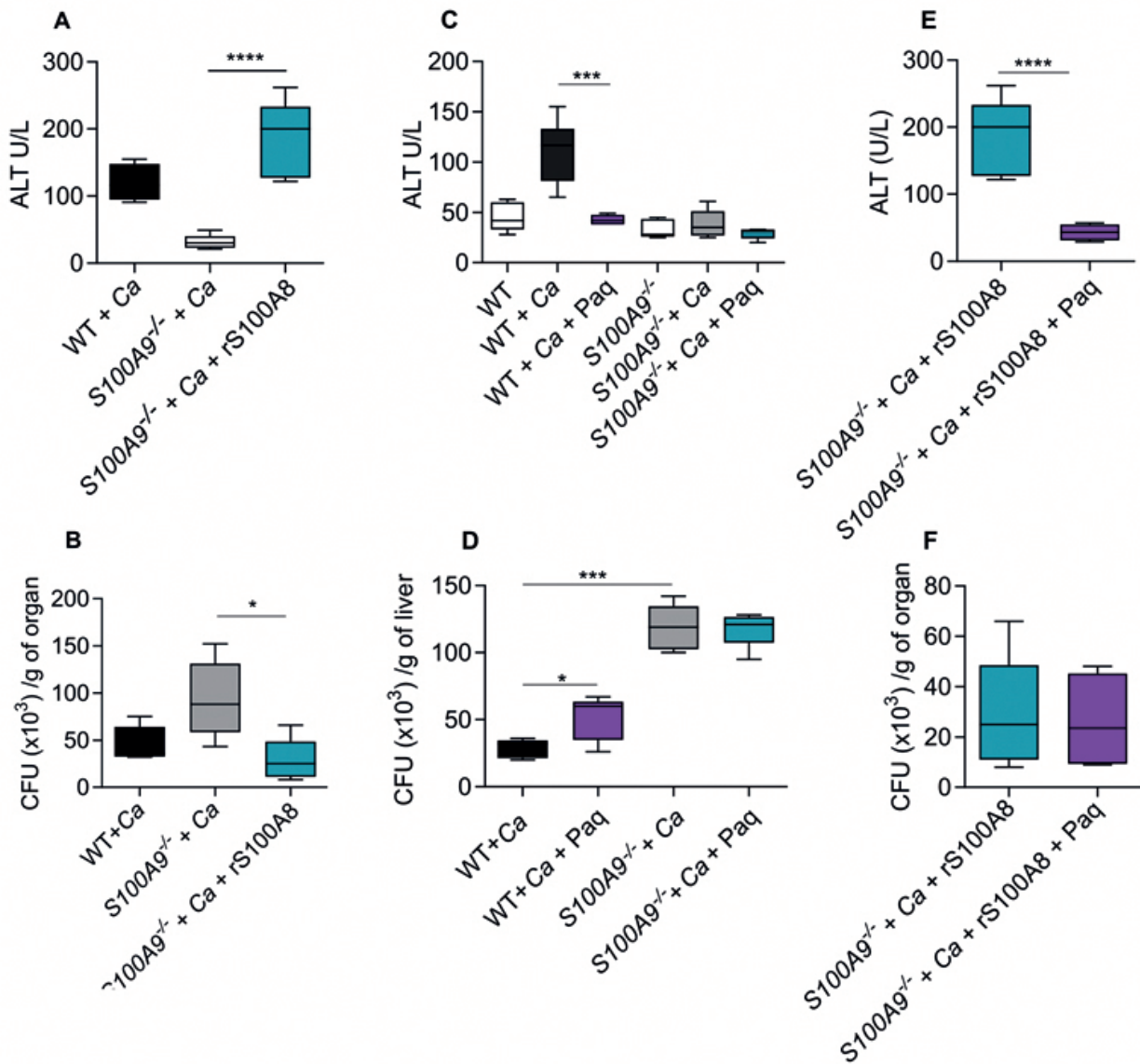
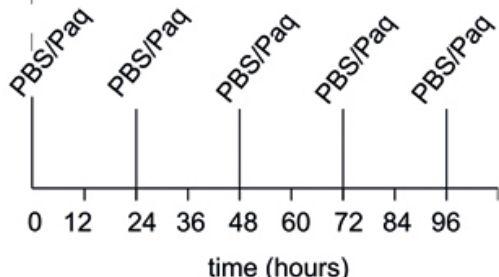


Figure 6 (Shankar et al. 2020)

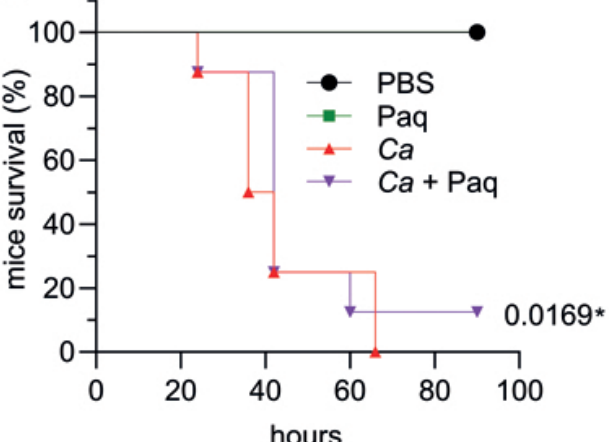
A

Single infection

C. albicans (Ca)



B



C

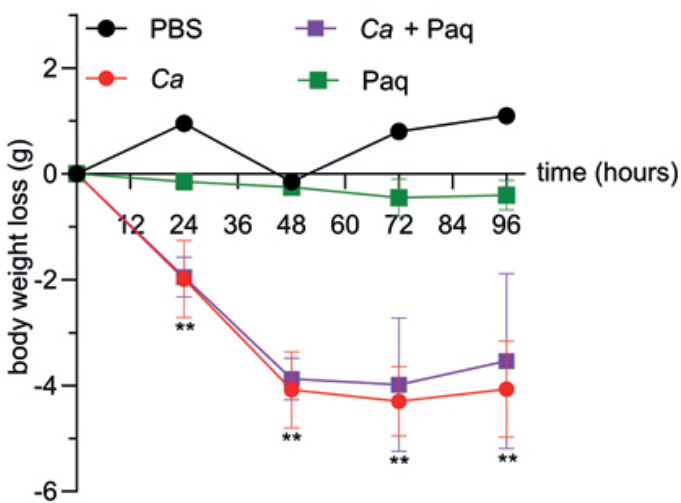


Figure 7 (Shankar et al. 2020)

